PLISKA

STUDIA MATHEMATICA BULGARICA

ПЛИСКА

БЪЛГАРСКИ МАТЕМАТИЧЕСКИ СТУДИИ

ANTI–PLANE SCATTERING BY HETEROGENEITIES IN PIEZOELECTRIC PLANE BY BIEM

Tsviatko Rangelov and Petia Dineva

ABSTRACT. Considered is homogeneous or functional graded piezoelectric material with heterogeneities of different type (hole, crack, inclusion, nano–hole, nano–inclusion) subjected to time–harmonic wave. With respect to the boundary conditions along the interface between the heterogeneity and the infinite matrix different boundary value problems are formulated and solved. Boundary Integral Equation Method is applied to evaluate both: (a) the wave far–field due to the wave scattering and diffraction; (b) the stress concentration field near heterogeneities.

The obtained results are applicable in the field of non–destructive testing, material science and fracture mechanics of multi–functional materials and structural elements based on them.

1. Introduction

Computational mechanics of multi–functional materials has a high priority in engineering society, because it concerns the development and creation of new smart materials and intelligent structures based on them. The field includes new mechanical models taking into consideration the role of the heterogeneity shape and size in macro and nano-scale range, the new type of the boundary conditions along the interfaces between the inhomogeneities and the matrix following by

corresponding computational techniques, software, new simulations and interpretation work.

The aim of this study is to propose an efficient boundary integral equation method (BIEM) for solution of 2D anti-plane dynamic problem of piezoelectric solids with heterogeneities of different type and size as macro (at length scales greater than $10^{-6}m$) and nano (within the interval $10^{-7}m$ to $10^{-9}m$) inclusions or holes. The modeling approach is in the frame of continuum mechanics of coupled fields, wave propagation theory, piezoelectricity and surface/interface elasticity theory of Gurtin and Murdoch [4]. Heterogeneities are considered in two aspects as wave scatters provoking scattered and diffraction wave fields and also as stress concentrators in the considered solid. The numerical modeling via BIEM has the potential to reveal the dependence of the scattered wave far-field and stress concentration near field on the electromechanical coupling, on the type and characteristics of the dynamic load, on the material characteristics and on the geometric shape and size of the heterogeneities.

2. Statement of the problem

In a Cartesian coordinate system Ox_1x_2 consider a bounded domain of an inclusion I with arbitrary shape with C^1 interface boundary $\partial I = S$ with an infinite piezoelectric matrix $M = R^2 \backslash I$, see Figure 2. The combined time–harmonic electro–mechanical load with a prescribed frequency ω is applied in the form of incident SH-wave in M and additionally electric load is applied on the boundary S. The displacements are: the anti–plane mechanical displacement $u_3^N(x, \omega)$ and the in-plane electrical displacements $D_j^N(x, \omega)$, $j = 1, 2$, $N = M, I$, $x = (x_1, x_2)$. The following notations are used: (a) for $x \in M$ we have $u_3^M(x, \omega), D_j^M(x, \omega)$; b) for $x \in I$ we have $u_3^I(x, \omega), D_j^I(x, \omega)$.

Heterogeneities can be inclusions or holes at macro and nanoscale.

2.1. Governing equations

The coupled field equations in absence of body forces consist of the following constitutive equations:

(1)
$$\sigma_{i3}^N = c_{44}^N s_{i3}^N - e_{15}^N E_i^N,$$

$$D_i^N = e_{15}^N s_{i3}^N + \varepsilon_{11}^N E_i^N,$$

the strain-displacement and electric field–potential relations:

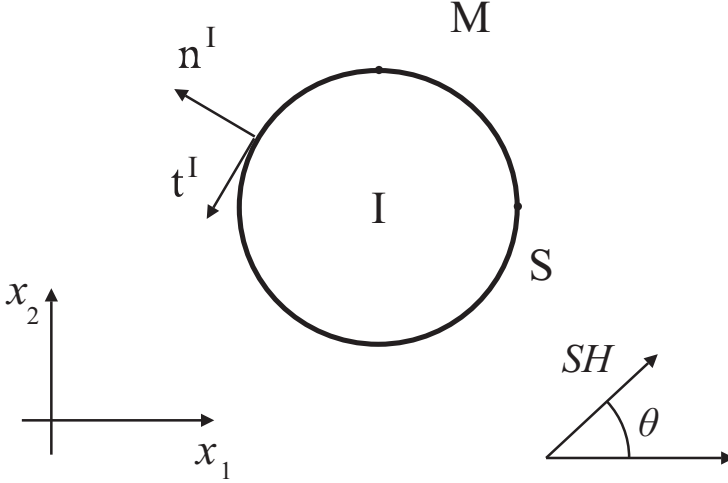(2)
$$s_{i3}^N = u_{3,i}^N, \quad E_i^N = -\phi_{,i}^N,$$

Figure 1- The geometry: PEM inclusion in an infinite PEM matrix under SH wave

and the balance equations in the frequency domain:

$$(3) \qquad \sigma^N_{i3,i} + \rho^N \omega^2 u^N_3 = 0, \quad D^N_{i,i} = 0.$$

Here $N = M, I$, σ^N_{i3}, s^N_{i3}, E^N_i, ϕ^N are the stress tensor, strain tensor, electric field vector and electric potential, respectively $i = 1, 2$; ρ^N is the mass density, c^N_{44} is the shear stiffness, e^N_{15} is the piezoelectric constant and ε^N_{11} is the dielectric permittivity for the matrix $N = M$, or inclusion $N = I$.

Let us introduce the notation of the generalized displacement as $u^N_J = (u^N_3, \phi^N)$, $J = 3, 4$, then the field equations are written in the following compact form

$$(4) \qquad \sigma^N_{iJ,i} + \rho^N_{JK} \omega^2 u^N_K = 0, \quad J, K = 3, 4, N = M, I,$$

where
(5)

$$\rho_{JK}^N = \begin{cases} \rho^N, & J = K = 3, \\ 0, & J = 4 \text{ or } K = 4, \end{cases} \qquad \sigma_{iJ}^N = \begin{cases} \sigma_{ij}^N, & J = 3, \\ D_i^N, & J = 4, \end{cases} \qquad \sigma_{iJ}^N = C_{iJKl}^N u_{K,l}^N,$$

$$C_{i33l}^N = \begin{cases} c_{44}^N, & i = l, \\ 0, & i \neq l, \end{cases} \qquad C_{i34l}^N = \begin{cases} e_{15}^N, & i = l \\ 0, & i \neq l, \end{cases} \qquad C_{i44l}^N = \begin{cases} -\varepsilon_{11}^N, & i = l \\ 0, & i \neq l. \end{cases}$$

2.2.   Electro–mechanical load

The electro–mechanical load u_J^{in} is composed by mechanical load u_J^{mech} in M and pure electrical load u_J^{el} on S, so $u_J^{in} = u_J^{mech} + u_J^{el}$ on S.

   The mechanical load is given by time-harmonic SH wave with an incident angle θ with respect to the x_1 axis. The generalized displacement u_J^{mech} due to this mechanical load satisfies the wave equation (4) for $N = M$, i.e. outside the heterogeneity. The generalized traction is $t_J^{mech} = C_{iJKl}^M u_{K,l}^{mech} n_i^M$, $n^M = (n_1^M, n_2^M)$ is the outward for the matrix M normal vector on S.

   Let us denote by $\eta = (\eta_1, \eta_2)$ the wave propagation vector, where $\eta_1 = \cos\theta$, $\eta_2 = \sin\theta$. Then the following expressions for the mechanically induced displacement components in the incident wave is obtained, see Shindo et al. [5]

(6)
$$u_3^{mech} = u_{03} e^{-ik^M \langle x, \eta \rangle}, \qquad u_4^{mech} = u_{03} \frac{e_{15}^M}{\varepsilon_{11}^M} e^{-ik^M \langle x, \eta \rangle}.$$

where u_{03} is the unit amplitude of the incident wave, $k^M = \sqrt{\dfrac{\rho^M}{c^M}}\omega$ and $c^M = c_{44}^M + \dfrac{(e_{15}^M)^2}{\varepsilon_{11}^M}$ and $\langle .., .. \rangle$ means the scalar product in R^2. The corresponding incident traction on the interface S is

(7)
$$t_3^{mech} = -ik^M c^M u_{03} \langle \eta, n \rangle e^{-ik\langle x, \eta \rangle}, \qquad t_4^{mech} = 0.$$

An applied time-harmonic pure electric in-plane load with an magnitude E_0 along the interface S induces electrically reduced generalized displacement components

(8)
$$u_3^{el} = 0, \qquad u_4^{el} = -E_0 \langle x, \eta \rangle.$$

The corresponding applied traction t_J^{el} along the interface S is

(9)
$$t_3^{el} = -e_{15}^M E_0 \langle n^M, \eta \rangle, \qquad t_4^{el} = \varepsilon_{11}^M E_0 \langle n^M, \eta \rangle.$$

The incident generalized displacement and traction fields on the interface boundary S can be presented as a superposition of the incident filed due to the propagating SH–wave and applied electrical load along this boundary.

$$(10) \qquad u_J^{in} = u_J^{mech} + u_J^{el}, \qquad t_J^{in} = t_J^{mech} + t_J^{el}.$$

The total generalized displacement and traction fields inside the matrix M and along the interface boundary S taking into consideration the scattered by the heterogeneities waves are

$$(11) \qquad u_J^{M} = u_J^{in} + u_J^{M,sc}, \qquad t_J^{M} = t_J^{in} + t_J^{M,sc},$$

while inside the heterogeneity I and along the interface S the corresponding total wave field is

$$(12) \qquad u_J^{I} = u_J^{I,sc}, \qquad t_J^{I} = t_J^{I,sc},$$

2.3. Boundary conditions

The BVPs are defined for the vector–function, displacement $u_J(x,\omega)$ denoted by

$$u_J(x,\omega) = \begin{cases} u_J^{M}(x,\omega), & x \in M \\ u_J^{I}(x,\omega), & x \in I \end{cases} \quad \text{where } u_J(x,\omega) \text{ satisfies (4) for } u_J^{M}(x,\omega)$$

inside the matrix M and for $u_J^{I}(x,\omega)$ inside the inclusion I. On the interface boundary S the displacement is continuous, i.e.

$$(13) \qquad u_J^{M}(x,\omega) = u_J^{I}(x,\omega), \quad \text{for} \quad x \in S.$$

The generalized traction on S is defined in two ways: first, using the stress σ_{iJ}^{M} in M and normal vector n^M on S, then $t_J^{in} + t_J^{sc} = t_J^{M} = \sigma_{iJ}^{M} n_i^{M}$, and second using the stress σ_{iJ}^{I} in I and normal vector n^I on S, then $t_J^{I} = \sigma_{iJ}^{I} n_i^{I}$.

For the considered anti–plane piezoelectric problem there are in general two types of boundary conditions on S for generalized stresses or traction, depending on the size of the heterogeneity.

2.3.1. Heterogeneity of nano–scale

In this case the interface equilibrium conditions along the undeformed interface boundary should take into consideration the surface effect appearing due to the nano-size of the inclusion, see Fang et al. [2]

$$(14) \qquad t_J^{M}(x,\omega) + t_J^{I}(x,\omega) = F^{S}(x,\omega) \neq 0, \quad \text{for} \quad x \in S.$$

where $F^S(x, \omega)$ is determined following the theory of Gurtin and Murdoch [4] and it will be specified below.

Since S is C^1 curve, then in every point $x \in S$ there are defined two unit vectors: outward normal $n^N(x)$ (i.e., directed out of the domain N, where $N = M$ or I and the corresponding tangent vector $l^N(x)$ directed such that the domain remains to the right hand side. For the stress on S at every point is defined normal and tangential stress as:

$$(15) \qquad t_J^N = \sigma_{nJ}^N = \langle \sigma_J^N, n^N \rangle, \quad \sigma_{lJ}^N = \langle \sigma_J^N, l^N \rangle$$

here stress $\sigma_J^N = (\sigma_{1J}^N, \sigma_{1J}^N)$, $J = 3, 4$ means the limit of the stress in domain N over S.

Tangential derivative of the tangential stress is defined as

$$(16) \qquad \langle \nabla \sigma_{lJ}^N, l \rangle = \frac{\partial \sigma_{lJ}^N}{\partial l}.$$

Denote with super–index S the displacement and the stress on S and let the constitutive equation for the surface stress and surface displacement, see Gurtin and Murdoch [4], Fang et al. [2] is given by

$$(17) \qquad \sigma_{pK}^S = C_{pKJj}^S u_{J,j}^S = C_{pKJj}^S u_{J,j}^M,$$

where for the last equality we use (13). In the mechanical model of Gurtin and Murdoch [4], the interface between the nano–inhomogeneity and the surrounding matrix is regarded as a thin membrane that possesses its own mechanical properties and own surface tension. The boundary conditions with accounting for the surface effect is given as:

$$(18) \qquad \sigma_{nJ}^I - \sigma_{nJ}^M = \frac{\partial \sigma_{lJ}^S}{\partial l}.$$

Note that at zero membrane interface parameters, the boundary condition (18) transforms into the classical boundary equilibrium condition for traction continuity. Also, in the case of nano–hole the first term in (18) is equal to zero.

2.3.2. Heterogeneity of macro-scale

In this case the classical equilibrium boundary condition along the interface boundary is satisfied, see Shindo et al. [5]

   - for inclusion

$$(19) \qquad t_J^M(x, \omega) + t_J^I(x, \omega) = 0, \quad \text{for} \quad x \in S.$$

- for hole

(20)
$$t_J^M(x, \omega) = 0, \quad \text{for} \quad x \in S.$$

2.4. Boundary value problems formulation

The following three BVP are defined due to different types of equilibrium boundary conditions for the stress:

A) Equations (4), (13) and (18) in the case of nano–inclusion/nano–hole;

B) Equations (4), (13) and (19) in the case of inclusion at macro scale;

C) Equations (4), (13) and (20) in the case of hole at macro scale.

Our aim is to solve both BVP A) and B) using the BIEM, see Dineva et al. [1]. The first step is to determine the displacement and the traction on the interface boundary S. The second step is using the boundary integral representation formulae to evaluate the displacement field inside the matrix M and inside the inclusion I as well as to compute the stress concentration factor (SCF) on S.

For the first step we have two vector–functions as unknowns: $u_J^{sc}(x, \omega)$ and $u_J^I(x, \omega)$ for $x \in S$ since $u_J^M(x, \omega) = u_J^{in}(x, \omega) + u_J^{sc}(x, \omega)$ for $x \in M$ and $u_J^{in}(x, \omega)$ is known for both BVP A) and B).

3. Fundamental solutions and derivatives

Fundamental solution of (4) is a matrix-value solution of the following partial differential equation

(21)
$$\Sigma_{iJQ,i}^{*,N}(x, \xi, \omega) + \rho_{JK}^N \omega^2 U_{KQ}^{*,N}(x, \xi, \omega) = -\delta_{JQ}\delta(x, \xi),$$

where $J, K = 3, 4, N = M, I$, δ_{JQ} is Kroneker symbol, $\delta(x, \xi)$ is Dirak's delta function, $\Sigma_{iJQ}^{*,N} = C_{iJKl}^N U_{KQ,l}^{*,N}$. The corresponding traction of the fundamental solution over the line with normal vector $n = (n_1, n_2)$ is defined as $T_{JQ}^{*,N}(x, \xi) = \Sigma_{iJQ}^{*,N} n_i$.

Proceeding as in Dineva et al. [1] we can find the fundamental solution using the Radon transform or the Fourier transform. In the present study we will apply the later method.

In a matrix and coordinate notations (21) has the form

$$c_{44}^N \Delta U_{33}^{*,N}(x,\xi) + e_{15}^N \Delta U_{43}^{*,N}(x,\xi) + \rho^N \omega^2 U_{33}^{*,N}(x,\xi) = -\delta(x,\xi),$$

$$c_{44}^N \Delta U_{34}^{*,N}(x,\xi) + e_{15}^N \Delta U_{44}^{*,N}(x,\xi) + \rho^N \omega^2 U_{34}^{*,N}(x,\xi) = 0,$$

(22)

$$e_{15}^N \Delta U_{33}^{*,N}(x,\xi) - \varepsilon_{11}^N \Delta U_{43}^{*,N}(x,\xi) = 0,$$

$$e_{15}^N \Delta U_{34}^{*,N}(x,\xi) - \varepsilon_{11}^N \Delta U_{44}^{*,N}(x,\xi) = -\delta(x,\xi).$$

where $\Delta = \dfrac{\partial^2}{\partial x_1^2} + \dfrac{\partial^2}{\partial x_2^2}$ is Laplace operator, and we omit the super-index N for simplicity.

Multiplying the third equation in (22) by $\dfrac{e_{15}^N}{\varepsilon_{11}^N}$ and adding to the first equation we obtain Helmholtz equation for $U_{33}^{*,N}(x,\xi)$

(23) $$\Delta U_{33}^{*,N}(x,\xi) + k^{N2} U_{33}^{*,N}(x,\xi) = -\frac{1}{c^N}\delta(x,\xi),$$

where $k^{N2} = \dfrac{\rho^N}{c^N}\omega^2$, $c^N = c_{44}^N + \dfrac{(e_{15}^N)^2}{\varepsilon_{11}^N}$. Solution of (23), see Vladimirov [6] is

$$U_{33}^{*,N}(x,\xi) = \frac{i}{2\pi a} K_0(-ik^N r),$$

where $r = \sqrt{(x_1 - \xi_1)^2 + (x_2 - \xi_2)^2}$ and $K_0(z)$ is Kelvin function of 0 order, see Gradshteyn and Ryzhik [3]. Using the equations (23) we obtain for the other elements of the matrix of fundamental solution

$$U_{43}^{*,N}(x,\xi) = U_{34}^{*,N}(x,\xi) = \frac{e_{15}^N}{\varepsilon_{11}^N} U_{33}^{*,N}(x,\xi);$$

$$U_{44}^{*,N}(x,\xi) = \left(\frac{e_{15}^N}{\varepsilon_{11}^N}\right)^2 U_{33}^{*,N}(x,\xi) + \frac{1}{2\pi\varepsilon_{11}^N}\ln r.$$

The kernels of the boundary integral equations discussed in Section 4. and describing the BVPs A), B) and C) are linear combination of $U_{JK}^{*,N}(x,\xi)$, $T_{JK}^{*,N}(x,\xi)$ on the line with normal vector n and $\Sigma_{iJK}^{*,N}(x,\xi)$ and their derivatives up to 2-nd

order. Using the recurrent relations for Kelvin functions, see Gradshteyn and Ryzhik [3] we obtain the following formulae

$$
(24) \quad
\begin{aligned}
U_{33,j}^{*,N}(x,\xi) &= \frac{ik^N}{2\pi c^N} K_1(-ik^N r) r_{,j}; \\[2mm]
&= \frac{-k^{N2}}{2\pi c^N} \left[K_2(-ik^N r)(r_{,j} r_{,l} - 0.5\delta_{jl}) + 0.5 K_0(-ik^N r)\delta_{jl} \right];
\end{aligned}
$$

$$
(25) \quad \Sigma_{j33}^{*,N}(x,\xi) = c^N U_{33,j}^{*,N}(x,\xi), \quad \Sigma_{j34}^{*,N}(x,\xi) = \frac{e_{15}^N}{\varepsilon_{11}^N} \left[c U_{33,j}^{*,N}(x,\xi) + \frac{1}{2\pi}(\ln r)_{,j} \right];
$$

$$
\Sigma_{j43}^{*,N}(x,\xi) = 0, \quad \Sigma_{j44}^{*,N}(x,\xi) = -\frac{1}{2\pi}(\ln r)_{,j}.
$$

$$
(26) \quad T_{33}^{*,N}(x,\xi) = c^N U_{33,j}^{*,N}(x,\xi) n_j, \quad T_{34}^{*,N}(x,\xi) = \frac{e_{15}^N}{\varepsilon_{11}^N} \left[c^N U_{33,j}^{*,N}(x,\xi) + \frac{1}{2\pi}(\ln r)_{,j} \right] n_j;
$$

$$
T_{43}^{*,N}(x,\xi) = 0, \quad T_{44}^{*,N}(x,\xi) = -\frac{1}{2\pi}(\ln r)_{,j} n_j.
$$

4. Boundary integral equations

Using the Gauss theorem and proceeding as in Dineva et al. [1] for the BVPs A), B) and C) a system of integro–differential equations (IDE) for the unknowns on S are obtained. The direct BIEM is developed, employing fundamental solutions of the Navier-Cauchy equations of dynamic equilibrium for the bulk solid.

4.1. BVP A) - for nano–heterogeneity

We will form 3 IDE for the unknowns on S: $u_J^{M,sc}$, $t_J^{M,sc}$ and t_J^I. Note here that in the case of nano-hole the last one is zero.

In the matrix M the displacement BIE is

$$
(27) \quad
\begin{aligned}
0.5 u_J^{M,sc}(x) &= -\int_S T_{KJ}^{*,M}(x,\xi) u_K^{M,sc}(\xi) d\xi \\[2mm]
&\quad + \int_S U_{KJ}^{*,M}(x,\xi) t_K^{M,sc}(\xi) d\xi, \quad x \in S.
\end{aligned}
$$

In the inclusion I the displacement IDE is

$$(28) \qquad 0.5u_J^I(x) = -\int_S T_{KJ}^{*,I}(x,\xi)u_K^I(\xi)d\xi + \int_S U_{KJ}^{*,I}(x,\xi)t_K^I(\xi)d\xi \quad x \in S.$$

From the boundary condition (13) now (28) becomes

$$0.5(u_J^{M,sc}(x) + u_J^{in}(x)) = -\int_S T_{KJ}^{*,I}(x,\xi)(u_K^{M,sc}(\xi) + u_K^{in}(\xi))d\xi$$

(29)

$$+ \int_S U_{KJ}^{*,I}(x,\xi)t_K^I(\xi)d\xi, \quad x \in S.$$

Applying the boundary condition (18) we obtain

$$t_J^I = -t_J^M + \langle (C_{kJQp}^S u_{Q,p}^M l_k), l \rangle$$

(30)

$$= -t_J^{in} - t_J^{sc} + \langle (C_{kJQp}^S (u_{Q,p}^{in} + u_{Q,p}^{M,sc}) l_k), l \rangle.$$

So, the system of IDE for the unknowns $u^{M,sc}$ and $t^{M,sc}$ on S becomes: (27) and (29) with the replacement (30).

4.2. BVP B) - for heterogeneity at macro–scale

In this case the unknowns are $u_J^{M,sc}$, $t_J^{M,sc}$ we use only equations (27), (29), replacing $t_J^I = -t^{in} - t^{M,sc}$.

4.3. BVP C) - for hole at macro–scale

In this case the unknown is $u_J^{M,sc}$, and we use equation (27) replacing $t_J^{M,sc} = -t^{in}$.

5. Numerical realization

5.1. Numerical scheme

The numerical solution procedure follows Dineva et al. [1]. Note that in the numerical scheme we have to use quadratic or higher order BE and shifted point method to have only CPV singular integrals in the integral equations. The following steps of the numerical procedure are realized:

(a) discretization by the usage of parabolic approximation of the unknowns;

(b) collection method along all boundary nodes;

(c) analytical solution of integrals with singular kernels based on the asymptotic behavior of the fundamentals solution and its derivatives for small arguments;

(d) solution of the algebraic system according to the unknowns along the interface S:

(e) computation of the displacement and traction at any point in the PEM plane by the usage of the integral representation formulae;

(f) SCF computation;

(g) creation of validated software based on Mathematica and Matlab.

Following [5] and [1], the dynamic SCF and electric field concentration factor along the perimeter of an inclusion is defined as the ratio of the stress and electric field amplitude along the circumference to the maximum amplitude of the incident stress at the same point in the homogeneous material without any defects.

The normalized dynamic SCF $|\sigma_{\gamma\theta}/\tau_0|$ and the normalized dynamic EFCF $|e_{15}E_{\gamma\theta}/\tau_0|$ are calculated by using the following formulae:

$$\sigma_{\theta\gamma} = -\sigma_1 \sin(\theta - \gamma) + \sigma_2 \cos(\theta - \gamma), \quad \sigma_i = \sigma_{i3} + \sigma_{i3}^{in},$$

(31)
$$E_{\theta\gamma} = -E_1 \sin(\theta - \gamma) + E_2 \cos(\theta - \gamma),$$

$$E_i = \frac{e_{15}}{e_{15}^2 + c_{44}\varepsilon_{11}}(-e_{15}\sigma_i + c_{44}D_i), \quad D_i = \sigma_{i4} + \sigma_{i4}^{in}.$$

Here τ_0 is the amplitude of the maximal shear stress of the incident plane SH-wave, i.e. $\tau_0 = i\omega\sqrt{c\rho}$, where γ is the angle of the observation point, θ is the incident wave angle and $c = c_{44} + \frac{e_{15}^2}{\varepsilon_{11}}$.

5.2. Validation

In this section is discussed the validation of the applied numerical solution of the BVP C. Considered is a circular hole embedded in a piezoelectric plane, which is loaded by a mechanical SH-wave, propagating in positive Ox_1 direction in conjunction with a time-harmonic electrical in-plane load $E_1 = E_0e^{-i\omega t}$ and $E_2 = 0$, see [5].

Material parameters are for PZT4: elastic stiffness: $c_{44} = c_{44}^M = 2.56 \times 10^{10}\text{N/m}^2$; piezoelectric constant: $e_{15} = e_{15}^M = 12.7\text{C/m}^2$; dielectric constant:

$\varepsilon_{11} = \varepsilon_{11}^M = 64.6 \times 10^{-10}\text{C/Vm}$; density: $\rho = \rho^M = 7.5 \times 10^3\text{kg/m}^3$. A dimensionless frequency is introduced, defined as $\Omega = a\sqrt{\dfrac{\rho}{c_{44}}}\,\omega$, a is the radius of the hole centered at the origin, greater than 10^{-6}m.
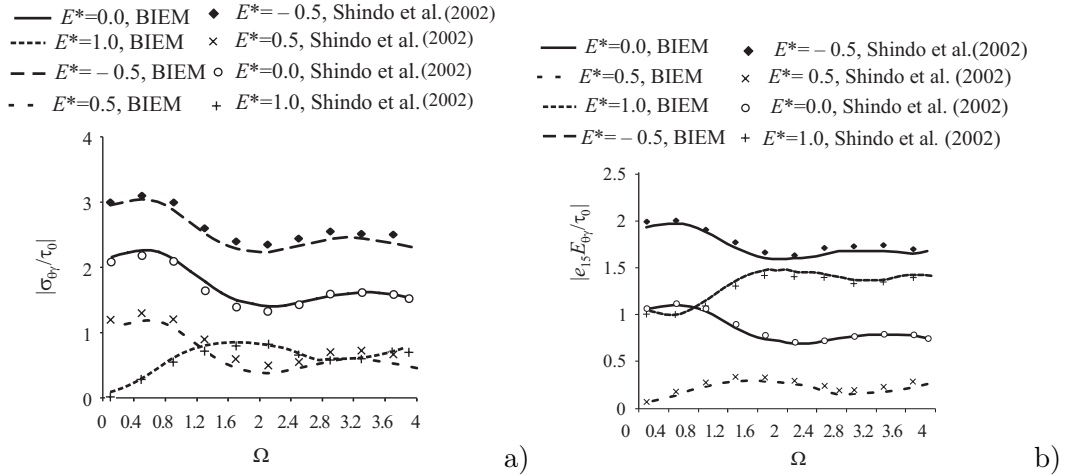

Figure 2 - Dynamic SCF a) and EFCF b) at observer point $A(0, c)$ versus normalized frequency Ω of the incident plane SH-wave with incident angle $\theta = 0$ for different electromechanical loads E^*.

A parameter $E^* = E_0\dfrac{e_{15}}{\tau_0}$ is used, where E_0 is the amplitude of the applied electrical load, in order to normalize appropriately the amplitude of the applied electrical field by the amplitude of the maximal shear stress of the incident SH-wave. The value of E^* is chosen to be $0.0, \pm 0.5$ and 1.0. Figure 2 a), b) shows a comparison of the results for the normalized generalized concentration field - SCF and EFCF versus normalized frequency Ω at the observation point $A(0, c)$ for all four values of E^*. As can be seen, the BIEM results agree very well with those of [5]. The difference of both results is below 7%, indicating a high accuracy of the obtained solution.

6.   Conclusion

Considered is homogeneous piezoelectric material with heterogeneities of different type (hole, inclusion, nano–hole, nano–inclusion) subjected to time-harmonic electro-mechanical load. With respect to the boundary conditions along the interface between the heterogeneity and the matrix different boundary value prob-

lems are formulated by the usage of BIE. Boundary Integral Equation Method is applied to evaluate both (*) the wave far-field due to the wave scattering and diffraction and (**) the stress concentration field near heterogeneities. The obtained results are applicable in the field of non-destructive testing and fracture mechanics of multi–functional materials and structural elements based on them.

The BIEM demonstrates the following advantages in comparison with the other computational techniques: (a) the semi-analytical character of the method as far as it is based on the fundamental solution of the considered problem; (b) high level of accuracy is achieved since numerical quadrature techniques are directly applied to the boundary integral equations, which are an exact solution of the considered problem; (c) the method is mesh reducing computational tool as far as the discretization is only along the interface in the considered problem; (d) flexibility to model solids containing heterogeneities of different geometrical shapes; (e) reduce the size of the problem dimensionality and the size of the resulting algebraic system in contrast to other domain discretization methods; (f) high accuracy and efficiency for evaluation of stress concentration fields because not mesh discretization is used close to the heterogeneity, but it is used the integral representations for the stress and displacement.

References

[1] P. Dineva, D. Gross, R. Müller, and T. Rangelov. *Dynamic Fracture of Piezoelectric Materials. Solutions of Time-harmonic problems via BIEM.* Solid Mechanics and its Applications, v. 212, Springer Int. Publ., Switzerland, 2014.

[2] X. Q. Fang, J. X. Liu, L. H. Dou, and M. Z. Chen. Dynamic strength araund two interacting piezoelectric nano–fibers with surfaces/interfaces in solid under electro–elastic wave. *Thin Solid Films*, 520:3587–3592, 2012.

[3] I. S. Gradshteyn and I. M. Ryzhik. *Tables of Integrals, Series, and Products.* Academic Press, New York, 1965.

[4] M. E. Gurtin and A. I. Murdoch. A continuum theory of elastic material surfaces. *Arch. Ration. Mach. Anal.*, 57:291–323, 1975.

[5] Y. Shindo, H. Moribayashi, and F. Narita. Scattering of antiplane shear waves by a circular piezoelectric inclusion embedded in a piezoelectric medium subjected to a steady-state electrical load. *ZAMM-Z. Angew.Math. Mech.*, 82: 43–49, 2002.

[6] V. Vladimirov. *Equations of Mathematical Physics.* Marcel Dekker, Inc., New York, 1971.

Tsviatko Rangelov
Institute of Mathematics and Informatics
Acad. G. Bonchev Str. Bl. 8
1113 Sofia, Bulgaria
e-mail:rangelov@math.bas.bg

Petia Dineva
Institute of Mechanics
Acad. G. Bonchev Str. Bl. 4
1113 Sofia, Bulgaria
e-mail:petia@imbm.bas.bg